

ELEVENTH EUROPEAN ROTORCRAFT FORUM

Paper No. 26

FINITE-TIME ARBITRARY-MOTION UNSTEADY CASCADE
AIRFOIL THEORY FOR HELICOPTER ROTORS IN HOVER

M.A.H. Dinyavari and P.P. Friedmann
Mechanical, Aerospace and Nuclear Engineering Department
University of California at Los Angeles
Los Angeles, California 90024, U.S.A.

September 10-13, 1985

London, England.

THE CITY UNIVERSITY, LONDON, EC1V 0HB, ENGLAND.

FINITE-TIME ARBITRARY-MOTION UNSTEADY CASCADE
AIRFOIL THEORY FOR HELICOPTER ROTORS IN HOVER*

M.A.H. Dinyavari[†] and P.P. Friedmann^{††}
Mechanical, Aerospace and Nuclear Engineering Department
University of California at Los Angeles
Los Angeles, California 90024, U.S.A.

ABSTRACT

A complete and detailed derivation of a finite-time arbitrary-motion cascade theory is presented for both Laplace and frequency domains. This theory includes the effect of returning wakes for both single- and multi-bladed rotors. The generalized cascade lift deficiency function, C'' , is shown to be consistent with the generalized Theodorsen's lift deficiency function when the wake spacing approaches infinity or when the reduced frequency tends to infinity. This function predicts correct zero-reduced-frequency limit. Accurate and efficient numerical procedures are presented for the evaluation of the cascade C'' . Numerical examples comparing the cascade lift deficiency function with Loewy's lift deficiency function in frequency domain are presented. Accurate Pade approximants of cascade lift deficiency function are constructed using Bode Plot approach which allows for complex poles.

Nomenclature

a	= Lower limit of integration for frequency domain cascade theory
a_m	= Coefficients in the numerator of the rational approximation for the lift deficiency function
$\bar{a}bR$	= Cross sectional elastic center (E.C.) offset from midchord
b_m	= Coefficients in the denominator of the rational approximation for the lift deficiency function
bR	= Blade semichord length
$C''(\bar{s}, \bar{T}_{Re}, \bar{T}_{He})$	= Cascade-wake lift deficiency function in the Laplace and frequency domains
$C''(ik, \bar{T}_{Re}, \bar{T}_{He})$	

* This research was supported by NASA Ames Research Center under NASA Grant NAG 2-209.

[†] Research Assistant and a Doctoral Candidate, presently Senior Dynamics Engineer, McDonnell Douglas Helicopter Company, Culver City, California.

^{††} Professor of Engineering and Applied Science.

$D(ik)$	= Denominator polynomial of rational approximation for the lift deficiency function
F'', G''	= Real and imaginary parts of cascade lift deficiency function
$F(\bar{s}; n, m, \bar{T}_R, \bar{T}_H)$	= Family of double integrals
F''_{app}, G''_{app}	= Real and imaginary parts of rational approximant to the lift deficiency function
$f_m(\bar{\phi})$	= Basis functions for the Glauert series
$\Delta h(t)$	= Vertical displacement of elastic center of the airfoil, positive downward
$h, h_e, \bar{h}, \bar{h}_e$	= Vertical wake spacing beneath the rotor in Loewy's model for single and multi-bladed rotors: $h_e = h/Q; h = [2\pi U_{p0}/\Omega]; (\bar{\quad}) = (\quad)/bR$
H^*, H_e^*	= Vertical wake spacing beneath the rotor in cascade wake model for single and multi-bladed rotor
$IMD(k)$	= Imaginary part of the denominator polynomial in a rational approximation to the lift deficiency function
$IMN(k)$	= Imaginary part of the numerator polynomial in a rational approximation to the lift deficiency function
i	= $\sqrt{-1}$
$I(t; n, m)$,	= The influence function of a vortex lying on the nth vortex sheet at ξ^* on the mth Fourier component of the wake induced downwash velocity λ_m
$IN(ik; n, m, \bar{T}_{Re}, \bar{T}_{He})$	= Family of double integrals associated with the numerator of the cascade-wake lift deficiency function
$ID(ik; n, m, \bar{T}_{Re}, \bar{T}_{He})$	= Family of double integrals associated with the denominator of the cascade-wake lift deficiency function
$K_n(\quad)$	= Modified Bessel function of the second kind of the order n
k	= Reduced frequency: $k = \omega b R / U_{T0}$

L, L_C, L_{NC}	= Total, circulatory and noncirculatory components of the lift
L_Q, L_W	= Quasisteady and wake components of the circulatory lift: $L_C = L_Q + L_W$
$N(ik)$	= Numerator polynomial of the rational approximation for the lift deficiency function
NL	= Number of wake layers beneath the rotor included in the cascade-wake lift deficiency function
NP	= Number of poles in the Pade approximant of the lift deficiency function
P	= Pressure
P_u, P_l	= Pressure on the upper and lower surfaces of the airfoil, respectively
$Q(t), Q(s)$	= Downwash velocity at the 3/4-chord point: $Q(s) = \mathcal{L}(Q(t))$
Q	= Number of blades
R	= Blade radius
$RD(k)$	= Real part of the denominator polynomial in a rational approximation for the lift deficiency function
$RN(k)$	= Real part of the numerator polynomial in a rational approximation for the lift deficiency function
$r, r_e, \bar{r}, \bar{r}_e$	= Radial station of blade section: $\bar{r}_e = (r/Q) = ()/bR$
s, \bar{s}	= Laplace transform variable: $\bar{s} = (sbR/U_{T0})$
T_H, T_{He}	= Time required for a fluid particle to travel one wake spacing with the mean oncoming flow velocity: $T_H = H^*/U_{T0}; T_{He} = H_e^*/U_{T0}$
T_R, T_{Re}	= Time required for a fluid particle to travel the distance between identical airfoils on consecutive blades with the mean oncoming flow velocity: $T_R = 2\pi r/U_{T0}; T_{Re} = 2\pi r_e/U_{T0}$

- T_{sc} = Time required for a fluid particle to travel the semichord length bR with the mean oncoming flow velocity:

$$T_{sc} = bR/U_{T0}$$
- $\bar{T}_H, \bar{T}_{He}, \bar{T}_R, \bar{T}_{Re}$ = Nondimensionalized T_H, T_{He}, T_R, T_{Re}
 With respect to T_{sc} : $(\bar{\quad}) = (\quad)/(T_{sc})$
- t, t', τ = Time
- $U_T(t), U_P(t)$ = Free stream velocity in x^* , and negative z^* directions respectively:

$$U_T(t) = U_{T0} + \Delta U_T(t); U_P(t) = U_{P0} + \Delta U_P(t)$$
- $W_a(x^*, \tau), W_a(\bar{\phi}, \tau)$ = Upwash velocity distribution over the airfoil
- $W_{am}(\tau)$ = Fourier coefficients of W_a
- $W_b(x^*, \tau), W_b(\bar{\phi}, \tau)$ = Downwash velocity distribution on the airfoil induced by the bound vortex system
- $X_0^*(\tau)$ = Location of trailing edge of the wake behind the reference airfoil at time

$$t = \tau$$
- $X_n^*(\tau)$ = Location of trailing edge of the wake behind the n th imaginary airfoil below the reference airfoil at time $t = \tau$ for cascade model
- x^*, z^* = Coordinate axes in plane of the airfoil
- X_A, \bar{X}_A = Offset between the elastic center and the aerodynamic center in blade cross section:

$$\bar{X}_A = X_A/bR$$

Greek Symbols

- $\alpha(t), \alpha_0, \Delta\alpha(t)$ = Time variant angle of incidence of the airfoil at the elastic center, measured clockwise from the horizontal x^* axis: $\alpha(t) = \alpha_0 + \Delta\alpha(t)$
- $\Gamma(\tau), \Gamma^{(1)}(\tau)$ = Various integrals of bound vortex over the airfoil in cascade-wake theory
 $\Gamma_{NC}^{(1)}(\tau), \Gamma_{NC}^{(2)}(\tau)$
 $\Gamma_C^{(1)}(\tau), \Gamma_C^{(2)}(\tau)$
- $\Gamma, \Gamma_Q, \Gamma_W$ = Total, quasisteady and wake induced circulation about the airfoil

$\gamma_a(\xi^*, \tau), \gamma_b(\xi^*, \tau)$	= Bound vortex strength distribution, positive clockwise
$\gamma_{bc}, \gamma_{bnc}$	= Circulatory and noncirculatory portions of bound vortex strength distribution
$\gamma_t(t')$	= Trailing edge vortex strength shed at time $t = t'$
$\gamma_{Wn}(\xi^*, \tau)$	= Shed wake vortex strength distribution, behind the n th imaginary airfoil at time $t = \tau$, positive clockwise
$\lambda(\xi^*, \tau)$	= Induced downwash velocity due to shed wakes behind and below the airfoil
$\lambda_m(\tau), \dot{\lambda}_m(\tau)$	= Fourier coefficients of the shed wake induced downwash velocity over the airfoil and its time derivative
$\xi^*(\tau, t', n)$	= Location of the vortex shed from behind the n th imaginary airfoil at time $t = t'$ observed at time $t = \tau$
ρ_A	= Air density
ψ	= Azimuth angle of blade measured from straight aft position, also nondimensional time: $\psi = \Omega t$
Ω	= Rotor speed of rotation

Special Symbols

∂	= Partial derivative
$\mathcal{L}\{ \}$	= Laplace transform
$(\dot{})$	= Differentiation with respect to time t

1. Introduction

Proper modeling of unsteady aerodynamic effects is an important ingredient in aeroelastic stability and response calculations for rotary wing applications. Until very recently all unsteady aerodynamic theories used in rotary-wing applications were based on the assumption of simple harmonic motion. An important shortcoming of these theories is that they are suitable only for determining aeroelastic stability boundaries, since the assumption of simple harmonic motion holds only at the stability boundaries. Therefore, these theories are not capable of predicting damping levels in the subcritical condition. Also, standard stability analysis techniques such as root locus method cannot be used in conjunction with these theories and special techniques representing variations of V-g method have to be devised. Furthermore, in the forward flight regime, where the blade equations of motion are governed by equations with periodic coefficients, the use of time domain unsteady aerodynamics is required for the inclusion of unsteady aerodynamic effects. Similarly the modeling of aeroservoelastic systems in which an active control system is modeled in conjunction with

the aeroelastic system, such as higher harmonic control system for vibration reduction in forward flight or for stability augmentation, requires finite-state time-domain unsteady aerodynamics.

In this paper the term finite-state time-domain aerodynamics refers to theories which express unsteady airloads in the time-domain in terms of a finite number of augmented state variables in addition to the airfoil (or blade) physical degrees of freedom. The role of these augmented state variables is to carry the effects of the unsteady wake. The term arbitrary finite-time motion is used here to refer to a motion which has commenced at some previous finite time and has an arbitrary form. The arbitrary form of motion includes both growing and decaying oscillations with a certain frequency.

In Reference 1, three incompressible finite-time arbitrary-motion airfoil theories, suitable for coupled flap-lag-torsional aeroelastic analysis of rotary wings in hover and forward flight were briefly outlined. These are:

- (1) A generalized version of Greenberg's² theory, which does not include the effect of returning wakes, and its finite-state time-domain approximation for hover and forward flight. This theory was also applied to a simple rotary wing aeroelastic problem in Ref. 3.
- (2) A generalized version of Loewy's theory⁴ and its finite-state time-domain approximation for hover. This theory includes the effects of the returning wakes beneath the rotor.
- (3) A generalized cascade theory with infinite or finite number of identical staggered airfoils flying beneath the reference blade, separated by appropriate wake spacing, for the case of hover. The airfoils of the cascade model represent wakes shed from the same blade in previous revolutions or different blades in the same revolution.

The generalized version of Greenberg's theory is restricted to a single unsteady wake layer which extends behind the airfoil for a length corresponding to the time elapsed from the beginning of motion. Although this theory is frequently used in rotary wing applications, it neglects the effect of returning wakes beneath the rotor. For low inflows the wakes shed from other blades in the same revolution and wakes shed in previous revolutions tend to remain in close vicinity of the rotor disk, and the effect of the returning wake has to be accounted for, particularly in the case of hover. The first theory to account for the influence of the layers of the shed⁴ vorticity beneath the rotor for the case of hover was developed by Loewy. This theory represents a generalization of Theodorsen's theory to rotary wing applications, and thus is based on the assumption of simple harmonic blade motion. The intertwined helical wakes (Fig. 1) shed by previous blades or the reference blade in previous revolutions was idealized by series of vortex sheets, infinite in number, parallel to rotor disk which extend to infinity on both sides of the airfoil representing a blade cross section, as shown in Fig. 2. Recently this theory was extended to the arbitrary motions in Refs. 1 and 5. However, it was pointed out in Refs. 1 and 5 that Loewy's wake model is not entirely compatible with the finite-time arbitrary-motion representation of the blade dynamics, because each

wake layer beneath the rotor is assumed to extend to infinity on both sides (Fig. 2). Thus, a generalized Loewy theory cannot be obtained from basic governing equations of fluid mechanics combined with the assumed wake model for this case. Furthermore, the techniques employed in Refs. 1 and 5 for constructing Pade approximants (a Pade approximant is the ratio of two polynomials in $i\omega$) for Loewy's lift deficiency function failed to capture the oscillatory behavior of the real and imaginary parts of this function. The techniques used in Refs. 1 and 5 were based on the assumption of real poles. In References 1 and 5 three different techniques were used to construct the Pade approximants for Loewy's lift deficiency function: (1) Dowell's quadratic least squares technique (Ref. 6), (2) Vepa's quadratic least squares technique (Ref. 7), and (3) General nonlinear least squares approach using Fletcher-Reeves unconstrained optimization algorithm.

In a recent study by Venkatesan and Friedmann the Bode plot was used to identify the number of complex poles and their approximate locations. High quality approximations to Loewy's lift deficiency function were obtained in Refs. 8 and 9. These approximations were successful in capturing the oscillatory behavior of Loewy's lift deficiency function. However, these approximations required the use of higher order polynomials.

This paper has a number of objectives: (1) to present a complete derivation of the finite-time arbitrary-motion cascade theory, which was briefly outlined in Ref. 1 and compare it to Loewy's theory (2) to develop an accurate finite-state time-domain representation of the loads using the improved Pade approximant technique developed in Refs. 8 and 9.

The results indicate that the lift deficiency function obtained for the cascade theory, are consistent with the generalized Theodorsen's lift deficiency function when the wake spacing approaches infinity, and when the complex reduced frequency approaches infinity. The cascade model always predicts the correct quasisteady loads for zero reduced frequency.

Accurate closed form binomial approximations are used to develop an efficient combined analytical and numerical technique for the evaluation of the lift deficiency function in the frequency domain. A detailed comparison of the cascade theory with Loewy's theory is presented.

Accurate Pade approximants of cascade lift deficiency function are constructed using the Bode plot approach described in Refs. 8 and 9 which allows for complex poles. The resulting approximate functions accurately model oscillatory behavior of lift deficiency function due to returning wakes.

2. Concise Derivation of the Cascade Theory

2.1 Overview of Wake Model

The finite-time cascade wake model consists of a wake in which a finite number of identical staggered imaginary airfoils which are assumed to be flying beneath the rotor. A schematic representation of the wake models for single-bladed rotors and multi-bladed rotors where all blades perform the same motion (collective mode) are shown in Figs. 3 and 4. The cascade

wake model for finite-time arbitrary motion utilized in this derivation is very similar to the wake structure assumed by Hammond and Pierce¹⁰. Ref. 10 uses an acceleration potential approach to obtain the compressible unsteady aerodynamic loads acting on two dimensional rotor blade cross sections, undergoing simple harmonic motions in hover. In the finite-time cascade wake model each airfoil is leading the previous one by the distance $(2\pi r)/Q$. The wakes behind the reference airfoil and each of the imaginary airfoils are of finite length corresponding to the time elapsed since the motion has commenced.

Using this wake model the integral equation of downwash is formulated for an airfoil undergoing coupled flap-lag-torsional motion about a nonzero pitch angle in a stream having time-varying oncoming and inflow velocities. It should be mentioned that the position of shed vortices behind the airfoil in each parallel wake layer are assumed to be determined by the mean velocity, whereas their instantaneous velocity is given by the time-varying oncoming velocity. This is similar to the wake assumption made in the derivation of generalized Greenberg's theory, described in Refs. 1 and 5. Therefore, the fore and aft excursions of the wake are partially accounted for.

The approach used to formulate the integral equation of the downwash is similar to the approach used by Johnson to derive Theodorsen's theory (Sec. 10, Ref. 11). The integral equation of downwash is solved using Söhngen inversion integral and a Fourier series method.

The unsteady aerodynamic loads are obtained using the Laplace transform. The resulting generalized lift deficiency function is shown to be consistent with the generalized Theodorsen lift deficiency function when the wake spacing approaches infinity, and when the complex reduced frequency approaches infinity on the imaginary axis.

Next the generalized cascade lift deficiency function is specialized to the frequency domain. In the frequency domain the wake is restricted to vortices contained within an azimuth angle straddling the reference blade. Certain numerical aspects associated with the evaluation of the lift deficiency function are also discussed in detail in the paper. A more detailed derivation of the cascade theory is provided in Ref. 5.

2.2 Formulation of the Theory

The geometry of motion of a typical airfoil is shown in Fig. 5. The governing equations for this problem consist of the boundary condition of zero disturbance upstream at infinity, tangent flow velocity over the reference airfoil, Kutta condition at the trailing edge of the reference airfoil, zero pressure discontinuity on the wake, and the condition of conservation of circulation.

The condition of tangency of flow to the airfoil surface leads to an expression for the upwash velocity of fluid particles on the surface of the airfoil in a Fourier series form

$$W_a(\vec{\phi}, t) = \sum_{m=0}^{\infty} W_{am}(t) \cos(m\vec{\phi}) \quad (1)$$

where

$$W_{am}(t) = 0 \quad n \neq 0, 1$$

$$W_{a0}(t) = -U_T(t) \alpha(t) - \Delta \dot{h} + U_P(t) - \bar{a} (bR) \Delta \dot{\alpha}(t) \quad (2)$$

$$W_{a1}(t) = (bR) \Delta \dot{\alpha}(t)$$

and

$$\bar{\phi} = \cos^{-1} (x^*/bR); \quad (0 \leq \bar{\phi} \leq \pi, -bR \leq x^* \leq bR)$$

In addition to the upwash velocity $W_a(\bar{\phi}, t)$ at the reference airfoil, there is also a downwash velocity component $\lambda(x^*, t)$ due to the shed wake, $\gamma_{wn}(\xi^*, t)$, $n=0, NL$, and a downwash velocity component $W_b(x^*, t)$ due to vortices representing the airfoil surface (i.e., the bound vortex), $\gamma_b(\xi^*, t)$.

Using the Biot-Savart law gives

$$W_b(x^*, \tau) = (-1/2\pi) \int_{-bR}^{bR} [\gamma_b(\xi^*, \tau) / (\xi^* - x^*)] d\xi^* \quad (3)$$

$$\lambda(x^*, \tau) = (-1/2\pi) \sum_{n=0}^{NL} \int_{bR-2n\pi r}^{X_n^*(\tau)} \left\{ \gamma_{wn}(\xi^*, \tau) (\xi^* - x^*) / [(\xi^* - x^*)^2 + (nH^*)^2] \right\} d\xi^*$$

where H^* represents the dimensional wake spacing between successive wake layers. The wake airfoils are purely imaginary and are introduced only to model the effects due to their wake. In essence the imaginary wake airfoils are only visual aids to help one write a relationship between the vortex strength in the wake layers beneath the reference airfoil and the wake vortices directly behind it. These airfoils do not represent physical surfaces over which discontinuities are produced, nor is there a bound vortex system associated with these wake airfoils.

The flow tangency and Kutta conditions can be written as

$$(1/2\pi) \int_{-1}^1 [\gamma_b(\xi, \tau) / (\xi - x)] d\xi = - [W_a(\tau) + \lambda(\tau)] \quad (4)$$

$$\gamma_b(+1, \tau) = \text{finite}$$

where $\xi = (\xi^*/bR)$ and $x = (x^*/bR)$ are nondimensional chordwise variables.

Application of Söhngen inversion integral yields

$$\gamma_b(x^*, \tau) = (-2/\pi) \sqrt{(bR-x^*)/(bR+x^*)} \times \int_{-bR}^{bR} \sqrt{(bR+\xi^*)/(bR-\xi^*)} \left[-(W_a + \lambda) / (x^* - \xi^*) \right] d\xi^* \quad (5)$$

This leads to the solution of γ_b in a Glauert series form

$$\gamma_b(\bar{\phi}, \tau) = -2 \sum_{m=0}^{\infty} \left[\lambda_m(\tau) + W_{am}(\tau) \right] f_m(\bar{\phi}) \quad (6)$$

where

$$f_m(\bar{\phi}) = \begin{cases} \tan(\bar{\phi}/2) & m = 0 \\ \sin(m\bar{\phi}) & m \geq 1 \end{cases} \quad (7)$$

Hence the expression for the bound circulation Γ becomes

$$\Gamma = \int_{-bR}^{bR} \gamma_b(z^*, \tau) dz^* = -2\pi(bR) \left[(W_{a0} + 1/2W_{a1}) + (\lambda_0 + 1/2\lambda_1) \right] \quad (8)$$

The bound vortex γ_b can be separated into two parts corresponding to a circulatory, γ_{bc} , and noncirculatory, γ_{bnc} , vortex distributions. The circulatory vortex, γ_{bc} , accounts for the total circulation around the airfoil, however it corresponds to zero downwash velocity, $W_b=0.0$, everywhere on the airfoil. Therefore the circulatory bound vortex system will have no effect on the flow tangency boundary condition over the airfoil, except at the trailing edge. The noncirculatory vortex system, γ_{bnc} , accounts for the total downwash velocity over the airfoil, however it produces zero circulation Γ around the airfoil.

Hence the following mathematical expressions can be written

$$\int_{-bR}^{bR} \gamma_{bc}(\xi^*, \tau) d\xi^* = \Gamma$$

$$\int_{-bR}^{bR} \gamma_{bnc}(\xi^*, \tau) d\xi^* = 0 \quad (9)$$

$$(1/2\pi) \int_{-bR}^{bR} \left[\gamma_{bc}(\xi^*, \tau) / (x^* - \xi^*) \right] d\xi^* = 0$$

$$(1/2\pi) \int_{-bR}^{bR} \left[\gamma_{bnc}(\xi^*, \tau) / (x^* - \xi^*) \right] d\xi^* = W_b(x^*, \tau) = -(W_a + \lambda)$$

This leads to

$$\begin{aligned}\gamma_{bc}(\bar{\phi}, \tau) &= [-2/\sin(\bar{\phi})] [(W_{a0} + 1/2W_{a1}) + (\lambda_0 + 1/2\lambda_1)] \\ \gamma_{bnc}(\bar{\phi}, \tau) &= [2/\sin(\bar{\phi})] [(W_{a0} + \lambda_0)\cos(\bar{\phi}) + 1/2(W_{a1} + \lambda_1)\cos(2\bar{\phi})] \\ &\quad - 2 \sum_{m=2}^{\infty} (W_{am} + \lambda_m) \sin(m\bar{\phi})\end{aligned}\quad (10)$$

The unsteady Bernoulli's equation can be used to obtain pressure difference ($P_u - P_l$) over the airfoil and expressions for the lift and moment

$$\begin{aligned}(P_u - P_l) &= -\rho_A \left[U_T(\tau) \gamma_b(x^*, \tau) + \frac{\partial}{\partial \tau} \int_{-bR}^{x^*} \gamma_b(\xi^*, \tau) d\xi^* \right] \\ L(\tau) &= \int_{-bR}^{bR} -(P_u - P_l) dx^* = \rho_A \left\{ U_T(\tau) \Gamma(\tau) - \frac{d}{d\tau} \left[\Gamma_{NC}^{(1)}(\tau) - \Gamma_C^{(1)}(\tau) \right] \right\} \\ M(\tau) &= \int_{-bR}^{bR} (P_u - P_l) (x^* - \bar{a} bR) dx^* = -\rho_A \left\{ U_T(\tau) \Gamma^{(1)}(\tau) \right. \\ &\quad \left. - 1/2 \frac{d}{d\tau} \left[\Gamma_{NC}^{(2)}(\tau) + \Gamma_C^{(2)}(\tau) \right] \right\}\end{aligned}\quad (11)$$

where the lift L and moment M are defined positive when they are acting in the upward and pitch-up directions, respectively.

The lift and moment expressions are expressed in terms of various integrals of bound vortex Γ , $\Gamma^{(1)}$, $\Gamma_{NC}^{(1)}$, $\Gamma_C^{(1)}$, $\Gamma_{NC}^{(2)}$ and $\Gamma_C^{(2)}$. These expressions together with certain auxiliary relations are provided below

$$\begin{aligned}\Gamma(\tau) &= \int_{-bR}^{bR} \gamma_{bc}(\xi^*, \tau) d\xi^* = -(2\pi)(bR) [(W_{a0} + 1/2W_{a1}) + (\lambda_0 + 1/2\lambda_1)] \\ \Gamma^{(1)}(\tau) &= \int_{-bR}^{bR} (\xi^* - \bar{a}bR) \gamma_b(\xi^*, \tau) d\xi^* = -(2\pi)(bR)^2 \left\{ -(1/2 + \bar{a}) \right. \\ &\quad \left. \left[(W_{a0} + 1/2W_{a1}) + (\lambda_0 + 1/2\lambda_1) \right] + (1/4) \left[(W_{a1} + W_{a2}) + (\lambda_1 + \lambda_2) \right] \right\} \\ \Gamma_{NC}^{(1)}(\tau) &= \int_{-bR}^{bR} \xi^* \gamma_{bnc}(\xi^*, \tau) d\xi^* = (2\pi)(bR)^2 \left[(1/2)(W_{a0} - 1/2W_{a2}) \right. \\ &\quad \left. + (1/2)(\lambda_0 - 1/2\lambda_2) \right]\end{aligned}\quad (12a)$$

$$\begin{aligned}
\Gamma_C^{(1)}(\tau) &= \int_{-bR}^{bR} (bR - \xi^*) \gamma_{bc}(\xi^*, \tau) d\xi^* = (bR) \Gamma(\tau) \\
\Gamma_{NC}^{(2)}(\tau) &= \int_{-bR}^{bR} (\xi^{*2} - 2\bar{a}bR) \gamma_{bnc}(\xi^*, \tau) d\xi^* = -(2\pi)(bR)^3 \\
&\quad \left\{ \bar{a} \left[(W_{a0} - 1/2W_{a2}) + (\lambda_0 - 1/2\lambda_2) \right] - (1/8) \left[(W_{a1} - W_{a3}) + (\lambda_1 - \lambda_3) \right] \right\} \\
\Gamma_C^{(2)}(\tau) &= \int_{-bR}^{bR} (\xi^{*2} - 2\bar{a}bR) \gamma_{bc}(\xi^*, \tau) d\xi^* = (1/2)(bR)^2 \Gamma(\tau)
\end{aligned} \tag{12b}$$

2.3 Aerodynamic Loads in the Laplace Domain

The expressions for the unsteady air loads derived in the previous section are in terms of the Fourier coefficients of the induced downwash velocity and their time derivatives. In turn, the wake-induced downwash velocity is a function of the strength of the unsteady shed wake vortices in the wake layers behind and beneath the blade. The complete solution for the unsteady airloads requires the solution for the strength of the shed wake vortices.

The coefficients of the Fourier series representation of λ , are calculated using

$$\begin{aligned}
\lambda_m(\tau) &= (2/\pi) \int_0^\pi \lambda(\bar{\theta}, \tau) \cos(m\bar{\theta}) d\bar{\theta} \\
\lambda_0(\tau) &= (1/2) \lambda_m(\tau) \Big|_{m=0}
\end{aligned} \tag{13}$$

The coefficients λ_m are given as

$$\lambda_m(\tau) = (-1/bR\pi) \sum_{n=0}^{NL} \int_{bR - 2n\pi r}^{X_n^*(\tau)} I(\xi^*:n,m) \gamma_{wn}(\xi^*, \tau) d\xi^* \tag{14}$$

where the expression for the kernel function $I(\xi^*:n,m)$ is

$$I(\xi^*:n,m) = (bR/\pi) \int_0^\pi \left\{ \left[(\xi^* - bR \cos \bar{\theta}) \cos m\bar{\theta} \right] / \left[(\xi^* - bR \cos \bar{\theta})^2 + (nH^*)^2 \right] \right\} d\bar{\theta} \tag{15}$$

$I(\xi^*:n,m)$ is the influence function for a unit vortex lying on the n th vortex sheet at ξ^* on the m th Fourier coefficient of the wake-induced velocity over the airfoil chord.

The wake vortex $\gamma_{wn}(\xi^*, \tau)$ can be related to the vortex shed at the trailing edge γ_t at some previous time t' . The shed vortex γ_t is only a function of time. At time $t = \tau$, the vortex shed from the trailing edge of the airfoil at time $t=0$ on the n th wake layer is located at $X_n^*(\tau)$, which is given by

$$X_n^*(\tau) = bR - 2n\pi r + \int_0^\tau U_T(t') dt' \tag{16}$$

Also the location of a vortex shed from the trailing edge of the airfoil at some previous time $t=t'$, at time $t = \tau$ is given by $\xi^*(\tau, t', n)$

$$\xi^*(\tau, t', n) = bR - 2n\pi r + \int_{t'}^{\tau} U_T(t) dt \quad (17)$$

In all unsteady aerodynamic theories the tangent flow boundary condition is imposed on the X^* axis as opposed to the moving airfoil surface. In a manner consistent with this assumption, the time varying velocity term appearing in the positions of the wake vortices will be approximated by their mean value.

$$X_n^*(\tau) = bR - 2n\pi r + (\tau) U_{T0} \quad (18)$$

$$\xi_n^*(\tau, t', n) = bR - 2n\pi r + (\tau - t') U_{T0}$$

The condition of zero pressure discontinuity across the wake requires the vortices shed at the trailing edge to travel downstream with the time-varying freestream velocity. This condition will be imposed in its exact form.

$$d\xi^*/dt' = -U_T(t') \text{ or } d\xi^* = -U_T(t') dt' \quad (19)$$

Therefore

$$\lambda_m(\tau) = (-1/bR\pi) \sum_{n=0}^{NL} \int_0^{\tau} I[(\tau-t'):n, m] [\gamma_t(t') U_T(t')] dt' \quad (20)$$

$$\begin{aligned} \dot{\lambda}_m(\tau) &= (-1/bR\pi) \sum_{n=0}^{NL} \int_0^{\tau} \frac{\partial}{\partial(\tau)} \left\{ I[(\tau-t'):n, m] \right\} [\gamma_t(t') U_T(t')] dt' \\ &\quad - (1/bR\pi) I[t=0:0, m] [\gamma_t(\tau) U_T(\tau)] \end{aligned} \quad (21)$$

where

$$\begin{aligned} I[(\tau-t'):n, m] &= \left[T_{sc}/\pi \right] \times \\ &\int_0^{\tau} \left\{ \left[[(\tau-t') + (T_{sc}) - n(T_R) - (T_{sc}) \cos \bar{\theta}] \cos(m\bar{\theta}) \right] / \right. \\ &\quad \left. \left\{ [(\tau-t') + (T_{sc}) - n(T_R) - (T_{sc}) \cos \bar{\theta}]^2 + (nT_H)^2 \right\} \right\} d\bar{\theta} \end{aligned} \quad (22)$$

The parameters T_{sc} , T_R and T_H are introduced because of convenience; T_{sc} is the time required for a fluid particle to travel one semichord length with the velocity U_{T0} , $T_{sc} = [(bR)/U_{T0}]$, T_R is Period of rotation of the rotor, $T_R = (2\pi/\Omega) = (2\pi r/U_{T0})$, and T_H is the time required for a fluid particle to travel one wake spacing with the speed U_{T0} , $T_H = [H^*/U_{T0}]$.

Introduction of a new kernel function for $\dot{\lambda}_m$ and performing its integrations leads to

$$\dot{\lambda}_m(\tau) = \left[-U_T(\tau)/\pi(bR)^2 \right] \sum_{n=0}^{NL} \int_0^\tau D [(\tau-t'):n,m] \left[\dot{\gamma}_t(t') U_T(t') \right] dt' \quad (23)$$

$$-(m/\pi bR) \frac{d}{d\tau} \left[\Gamma(\tau) \right]$$

where

$$D [(\tau-t'):n,m] = \left[(T_{sc})^2/\pi \right] \int_0^\pi \left\{ (nT_H)^2 - [(\tau-t')+T_{sc} - nT_R - T_{sc} \cos\bar{\theta}]^2 \right\} /$$

$$\left\{ [(\tau-t')+T_{sc} - nT_R - T_{sc} \cos\bar{\theta}]^2 + (nT_H)^2 \right\}^2 \cos(m\bar{\theta}) d\bar{\theta}$$

$$D [(\tau-t'):n,m] = T_{sc} \frac{d}{d\tau} I [(\tau-t'):n,m] \quad (24)$$

The expression for the lift in terms of its quasisteady, noncirculatory and wake contributing becomes

$$L(\tau) = L_Q(\tau) + L_{NC}(\tau) + L_W(\tau) = L_C(\tau) + L_{NC}^{(\tau)} \quad (25)$$

where

$$\left[L_C(\tau)/2\rho_A U_T(\tau) \right] = (1/2) \int_0^\tau \left[\sum_{n=0}^{NL} \left\{ (1/2) D [(\tau-t'):n,0] \right. \right.$$

$$\left. \left. - (1/2) D [(\tau-t'):n,2] \right\} - 1 \right]$$

$$\left[\dot{\gamma}_t(t') U_T(t') \right] dt' \quad (26)$$

$$L_{NC}(\tau) = -(\pi)\rho_A (bR)^2 \dot{W}_{a0} \quad (27)$$

Using Helmholtz principle of conservation of the circulation, the following relation for quasisteady lift can be obtained

$$\begin{aligned} \left[L_Q(\tau) / 2\rho_A U_T(\tau) \right] = \pi(bR) Q(\tau) = - \int_0^\tau \left[\sum_{n=0}^{NL} \left\{ (1/2) I [(\tau-t') : n, 0] \right. \right. \\ \left. \left. + (1/2) I [(\tau-t') : n, 1] \right\} + (1/2) \right] \\ \left[\dot{\gamma}_t(t') U_T(t') \right] dt' \end{aligned} \quad (28)$$

where $Q(\tau)$ is the 3/4-chord-point downwash velocity given by

$$\begin{aligned} Q(\tau) = -(W_{a0} + 1/2 W_{a1}) = \left\{ U_T(\tau) [\alpha_o + \Delta\alpha(t)] \right. \\ \left. + \Delta h - U_p(t) + bR(1/2 - \bar{a}) \dot{\Delta\alpha}(t) \right\} \end{aligned} \quad (29)$$

It is important to note that both Eqs. (26) and (28) are in convolution form, and they both involve the unknown trailing edge vortex strength multiplied by the time-varying velocity, $[\dot{\gamma}_t(t') U_T(t')]$. Therefore the Laplace transformation can be used in order to eliminate the unknown $[\dot{\gamma}_t(t') U_T(t')]$.

$$\mathcal{L} \left[L_C(\tau) / 2\pi\rho_A (bR) U_T(\tau) \right] = C'' \mathcal{L} \{ Q(\tau) \} \quad (30)$$

where the generalized cascade lift deficiency function C'' which acts as a Laplace domain operator for the loads is given by

$$C'' = -(1/2) \left[\frac{\mathcal{L} \left\{ \sum_{n=0}^{NL} \left[(1/2) D(t:n, 0) - (1/2) D(t:n, 2) \right] - 1 \right\}}{\mathcal{L} \left\{ \sum_{n=0}^{NL} \left[(1/2) I(t:n, 0) + (1/2) I(t:n, 1) \right] + (1/2) \right\}} \right] \quad (31)$$

The expression for $C''(s)$ is further reduced in Ref. 5

$$C''(\bar{s}, \bar{T}_R, \bar{T}_H) = \left[K_1(\bar{s}) - (\bar{s}/2) \sum_{n=1}^{NL} e^{-n\bar{T}_R \bar{s}} \left[F(\bar{s}:n, 0, \bar{T}_R, \bar{T}_H) - F(\bar{s}:n, 2, \bar{T}_R, \bar{T}_H) \right] \right] / \left[\left[K_1(\bar{s}) + K_0(\bar{s}) \right] + \sum_{n=1}^{NL} e^{-n\bar{T}_R \bar{s}} \left[F(\bar{s}:n, 0, \bar{T}_R, \bar{T}_H) + F(\bar{s}:n, 1, \bar{T}_R, \bar{T}_H) \right] \right] \quad (32)$$

where the expression for $F(\bar{s}:n, m, \bar{T}_R, \bar{T}_H)$ is given by

$$F(\bar{s}:n, m, \bar{T}_R, \bar{T}_H) = \int_{1-n\bar{T}_R}^{\infty} \left[(1/\pi) \int_0^{\pi} \left[[t' - \cos\bar{\theta}] \cos(m\bar{\theta}) / \left\{ [t' - \cos\bar{\theta}]^2 + (n\bar{T}_H)^2 \right\} \right] d\bar{\theta} \right] e^{-\bar{s}t'} dt' \quad (33)$$

This Laplace-domain lift deficiency function involves two infinite summations and integrals which do not lend themselves to closed form solutions in terms of familiar mathematical functions. However several important properties of C'' can be analyzed analytically.

Reference 5 contains a mathematical proof that the limit of the lift deficiency function for the cascade-wake theory approaches Theodorsen's lift deficiency function when the wake spacing approaches infinity. It is also shown that the cascade theory becomes identical to the generalized Greenberg's theory (Ref. 5), when returning wake layers are neglected ($NL=0$).

The multibladed rotor is different from the single bladed rotor in that the horizontal shift between successive layers will be reduced. This new wake-layer shift is equal to the distance between two identical airfoils on successive blades. Furthermore, the wake spacing is also reduced by a factor equal to the total number of the blades of the rotor. Thus

$$\begin{aligned} \bar{T}_{Re} &= \bar{T}_R / Q \\ \bar{T}_{He} &= \bar{T}_H / Q \end{aligned} \quad (34)$$

3. Frequency Domain Lift Deficiency Function

Accurate evaluation of the frequency domain lift deficiency function for the cascade-wake theory is required, for several reasons. First, the lift deficiency function of the cascade-wake theory needs to be compared with Loewy's lift deficiency function in the frequency domain. Next it should be noted that finite state time domain models are based on the Pade approximants of the lift deficiency function developed for the frequency domain. In this section an efficient method for calculating the lift deficiency function for the cascade-wake theory in the frequency domain is presented.

3.1 Derivation

The frequency domain lift deficiency function can be obtained by replacing the nondimensional Laplace variable \bar{s} by (ik) . It is more convenient to treat the various integrals in the numerator and denominator of C'' separately. The combined integral for the numerator will be denoted by $IN(ik:n, \bar{T}_{Re}, \bar{T}_{He})$, and the combined integral for the denominator will be denoted as $ID(ik:n, \bar{T}_{Re}, \bar{T}_{He})$.

$$IN(ik:n, \bar{T}_{Re}, \bar{T}_{He}) = \int_{[1-n\bar{T}_{Re}]_0}^{\infty} \left[(1/\pi) \int_0^{\pi} \left[[t' - \cos\bar{\theta}] [1 - \cos(2\bar{\theta})] / \left\{ [t' - \cos\bar{\theta}]^2 + (n\bar{T}_{He})^2 \right\} \right] d\bar{\theta} \right] e^{-ikt'} dt' \quad (35)$$

$$ID(ik:n, \bar{T}_{Re}, \bar{T}_{He}) = \int_{[1-n\bar{T}_{Re}]_0}^{\infty} \left[(1/\pi) \int_0^{\pi} \left[[t' - \cos\bar{\theta}] [1 + \cos(\bar{\theta})] / \left\{ [t' - \cos\bar{\theta}]^2 + (n\bar{T}_{He})^2 \right\} \right] d\bar{\theta} \right] e^{-ikt'} dt' \quad (36)$$

It should be noted that the upper limits of the outer integrals in "IN" and "ID" are infinity. This indicates the wake is allowed to extend to infinity behind the imaginary airfoils. However only the wake contained within a double azimuth angle straddling the blade has physical meaning. An assumption will be made that only the vortices contained within a double azimuth angle $(2\pi/Q)$ straddling the reference blade are important for the wake layers beneath the rotor. Therefore the limits of integration for the outer integrals in IN and ID are adjusted so as to reflect this assumption. The physical regions of the wake layers beneath the reference airfoil lie on $-(2\pi r/Q) \leq \xi_n^* \leq (2\pi r/Q)$. A change of variables from position of vortices ξ_n^* on the n -th wake layer in a Q -bladed rotor, to a time variable t' can be obtained

$$\xi_n^* = bR - (2\pi rn/Q) + \Omega r t \quad (37)$$

$$t = T_{sc} [t' - (1-n\bar{T}_{Re})] \quad (38)$$

Using these relations, one obtains

$$\begin{aligned}\xi^* = 2\pi r/Q \text{ corresponds to } t' &= \bar{T}_{Re} \\ \xi^* = -2\pi r/Q \text{ corresponds to } t' &= -\bar{T}_{Re}\end{aligned}\tag{39}$$

Therefore, the limits of integration for outer integrals in IN and ID can be modified in the following manner

$$\begin{aligned}IN(ik:n, \bar{T}_{Re}, \bar{T}_{He}) &= \int_{-a}^{\bar{T}_{Re}} \left[(1/\pi) \int_0^\pi \left[[t' - \cos \bar{\theta}][1 - \cos(2\bar{\theta})] / \right. \right. \\ &\quad \left. \left. \{ [t' - \cos \bar{\theta}]^2 + (n\bar{T}_{He})^2 \} \right] d\bar{\theta} \right] e^{-ikt'} dt'\end{aligned}\tag{40a}$$

$$\begin{aligned>ID(ik:n, \bar{T}_{Re}, \bar{T}_{He}) &= \int_{-a}^{\bar{T}_{Re}} \left[(1/\pi) \int_0^\pi \left[[t' - \cos \bar{\theta}][1 + \cos(\bar{\theta})] / \right. \right. \\ &\quad \left. \left. \{ [t' - \cos \bar{\theta}]^2 + (n\bar{T}_{He})^2 \} \right] d\bar{\theta} \right] e^{-ikt'} dt'\end{aligned}\tag{40b}$$

where

$$a = \begin{cases} \bar{T}_{Re} & \text{for } n \neq 1 \\ \bar{T}_{Re}^{-1} & \text{for } n = 1 \end{cases}\tag{40c}$$

The integrands in "IN" and "ID" are well behaved and have no singularity in the region of the integration. Therefore, the integration in the rectangular region of $0 \leq \theta \leq \pi$, $-a \leq t' \leq \bar{T}_{Re}$ can be treated using any available numerical integration techniques, such as Gaussian quadrature or adaptive Romberg extrapolation algorithms.

3.2 Computational Aspects

In actual applications these integrals have to be evaluated numerically for a large number of wake layers at each reduced frequency k , and this calculation requires considerable amount of computer time to generate plots of C'' as a function of k . To reduce the computation time, approximate expressions replacing the integrands of IN and ID for wake layers sufficiently far from the rotor were developed. In Ref. 5 it was shown that the integrand of the outer integral in IN is an odd function of t' , and therefore IN for $n \neq 1$ reduces to

$$IN(ik:n, \bar{T}_{Re}, \bar{T}_{He}) = -(2i) \int_0^{\bar{T}_{Re}} \left[(1/\pi) \int_0^{\pi} \left[[t' - \cos\bar{\theta}][1 - \cos(2\bar{\theta})] / \right. \right. \\ \left. \left. \{ [t' - \cos\bar{\theta}]^2 + (n\bar{T}_{He})^2 \} \right] d\bar{\theta} \right] \sin(kt') dt' \text{ for } n \neq 1 \quad (41)$$

This equation reveals two separate important properties of IN:

- (1) "IN" approaches zero as k approaches either zero or infinity, irrespective of the wake layer index n, i.e.

$$\lim_{k \rightarrow 0} IN(ik:n, \bar{T}_{Re}, \bar{T}_{He}) = 0 \\ \lim_{k \rightarrow \infty} IN(ik:n, \bar{T}_{Re}, \bar{T}_{He}) = 0 \quad (42)$$

This property becomes important in determining the limiting values of C' as k approaches zero or infinity.

- (2) The real part of "IN" is always zero, and "IN" is purely an imaginary number.

For wake layers sufficiently far from the rotor disk a highly accurate closed form approximate solution can be obtained by using binomial expansion which eliminates the need for numerical integration (Ref. 5).

$$IN(ik:n, \bar{T}_{Re}, \bar{T}_{He}) = \left\{ 2i / (n\bar{T}_{He})^4 \right\} \times \\ \left[\left\{ \left[(n\bar{T}_{He})^2 - 3/4 \right] (1/k) + (6/k^3) \right\} \bar{T}_{Re} - (\bar{T}_{Re})^3/k \right\} \cos(k\bar{T}_{Re}) \\ - \left\{ \left[(n\bar{T}_{He})^2 - 3/4 \right] (1/k^2) + (6/k^4) - [3(\bar{T}_{Re})^2 / (k)^2] \right\} \sin k\bar{T}_{Re} \quad (43)$$

$$ID(ik:n, \bar{T}_{Re}, \bar{T}_{He}) = \left\{ 2 / (n\bar{T}_{He})^4 \right\} \times \left[[3\bar{T}_{Re} / k^2] \cos(k\bar{T}_{Re}) \right. \\ + \left\{ [-(1/2)(n\bar{T}_{He})^2 + (3/8)] (1/k) - (3/k^3) + (3\bar{T}_{Re}^2 / 2k) \right\} \cos(k\bar{T}_{Re}) \\ - i \left\{ [(n\bar{T}_{He})^2 - (3/2)] (1/k^2) + (6/k^4) - (3\bar{T}_{Re}^2 / k^2) \right\} \sin(k\bar{T}_{Re}) \\ \left. + i \left\{ [(n\bar{T}_{He})^2 - (3/2)] (\bar{T}_{Re} / k) + (6\bar{T}_{Re} / k^3) - (\bar{T}_{Re}^3 / k) \right\} \cos(k\bar{T}_{Re}) \right] \quad (44)$$

For an allowable upper-bound error of 1 percent, this approximation is valid for wake layers below nth wake layer.

$$n \geq [100]^{1/4} \left[[\bar{T}_{Re}] / [n\bar{T}_{He}] \right] \quad (45)$$

3.3 Comparison with Loewy's Theory

In this comparison two questions are addressed: 1) how does the cascade lift deficiency function vary with the number of wake layers? 2) how does the cascade wake theory differ from Loewy's theory throughout the complete range of reduced frequencies? The numerical results presented in this section provide useful insight to these questions.

The nondimensional horizontal wake shift and nondimensional vertical wake spacing parameters selected for the numerical examples presented in this paper are:

$$\bar{T}_{Re} = 9.4248, \bar{T}_{He} = 1.5707$$

This case corresponds to a blade section of radial distance $0.3R$ of a four bladed rotor with a semichord $bR = 0.05R$ operating at an inflow ratio of 0.05 or thrust coefficient of 0.005 . The corresponding parameters for Loewy's theory are:

$$\bar{r}_e = 1.500, \bar{h}_e = 1.5707$$

For this case the integer frequency ratio will occur at the reduced frequencies $k = 0.666, 1.333, 2.000, 2.666, \dots (0.666m)$, where m is any integer.

The real and imaginary parts of the cascade-wake lift deficiency function, for various values of reduced frequency, were calculated using a combined analytical/numerical method. The contributions of the first 20 wake layers were calculated using numerical integration, and approximate closed form solutions were used for the remaining wake layers. The real and imaginary parts of the cascade wake theory lift deficiency function are plotted against the reduced frequency in Figs. 6 and 7, respectively, for an increasing number of wake layers. The number of wake layers beneath the rotor disk, NL , has been varied from 0 to 100. The case without returning wake layers beneath the rotor, $NL = 0$, is identical to Theodorsen's theory. Figs. 6 and 7 show that there is a large difference due to the inclusion of the returning wakes (i.e., $NL > 0$). The effects of the first 20 returning wake layers are more pronounced than the remaining wake layers. In addition the imaginary part of the lift deficiency function seems to converge faster than the real part with increasing number of wake layers. More importantly the cascade lift deficiency function exhibits peaks and valleys in the vicinity of the reduced frequencies corresponding to the integer equivalent frequency ratios, for this case $k = 0.666, 1.333, 2.000, 2.666, \dots (0.666 m)$, where m is any integer.

It is also interesting to compare the cascade wake theory with Loewy's theory. The real and imaginary parts of the cascade lift deficiency function with 100 wake layers beneath the rotor are compared with Loewy's theory in Figs. 8 and 9, respectively. The cascade wake theory lift deficiency function agrees very well with Loewy's lift deficiency function except in two regions: 1) in the vicinity of the regions where $\bar{m}_e = (k)$. (\bar{r}_e is an integer and, 2) near the origin where the cascade wake theory tends to the correct quasi-steady value. From these plots it is also

evident that Loewy's lift deficiency function tends to reduce somewhat the effect of the returning wakes near the integer frequency ratios when compared with the cascade wake theory. One could speculate as to the possible cause for this difference. One possibility is that the extension of the wake to infinity on both sides of the rotor, as done in Loewy's theory, could lead to wake cancellations at integer frequency ratios and hence reduced unsteady effects. Despite this difference both theories indicate very large unsteady effects at integer frequency ratios.

It should also be noted that the zero-frequency limit of Loewy's lift deficiency function for this numerical example is $C' = (0.8667 + i 0.2667)$, corresponding to 9.32 percent reduction and 17.10° phase lead in circulatory loads. However, the generalized cascade lift deficiency function always approaches unity as reduced frequency goes to zero. The zero frequency limit for Loewy's lift deficiency function was calculated using the expressions derived in Refs. 1 and 5.

$$C' = F' + iG'$$

$$\lim_{|\bar{s}| \rightarrow 0} F' = \frac{\left[1 + \frac{\pi \bar{h}_e}{\bar{h}_e^2 + (2\pi \bar{r}_e)^2} \right]}{\left[1 + \frac{\pi \bar{h}_e}{\bar{h}_e^2 + (2\pi \bar{r}_e)^2} \right]^2 + \left[\frac{2\pi^2 \bar{r}_e}{\bar{h}_e^2 + (2\pi \bar{r}_e)^2} \right]^2}$$

$$\lim_{|\bar{s}| \rightarrow 0} G' = \frac{\left[\frac{(2\pi^2 \bar{r}_e)}{\bar{h}_e^2 + (2\pi \bar{r}_e)^2} \right]}{\left[1 + \frac{\pi \bar{h}_e}{\bar{h}_e^2 + (2\pi \bar{r}_e)^2} \right]^2 + \left[\frac{2\pi^2 \bar{r}_e}{\bar{h}_e^2 + (2\pi \bar{r}_e)^2} \right]^2}$$

(46)

4. Finite State Modeling of Cascade Lift Deficiency Function

The Bode plot of the cascade lift deficiency function is shown in Fig. 10. Ten peaks and valleys are identified in Fig. 10, the odd numbers correspond to the valleys and the even numbers correspond to the peaks. In References 8 and 9 the following rules have been utilized for locating the approximate location of complex poles and zeros. A -40 dB/decade change in slope in the asymptotes indicates the presence of either complex poles or two equal real poles and a +40 dB/decade change in slope indicates the presence of either complex zeros or two equal real zeros. Therefore each valley in the Bode plot indicates the presence of a pair of complex conjugate or repeated real zeros and each peak indicates the presence of a pair of complex conjugate or repeated real poles. In addition, whenever the slopes of the asymptotes of the transfer function are equal at low and high frequencies (i.e., zero and infinity) then the transfer function

has equal number of zeros and poles. Figure 10 shows five complex poles and five complex zeros for the cascade lift deficiency function in the frequency range of $0 \leq k \leq 3.0$. Furthermore the cascade lift deficiency function has a known branchcut on the negative real axis. Hence an approximate transfer function is constructed so as to capture the first five complex poles and zeros and the branchcut.

$$C''(ik, \bar{T}_{Re}, \bar{T}_{He}) = \frac{N(ik)}{D(ik)} = \frac{RN(k)+iIN(k)}{RD(k)+iID(k)} = 0.5 \frac{(ik)^{15} + \sum_{m=1}^{15} a_m (ik)^{(15-m)}}{(ik)^{15} + \sum_{m=1}^{15} b_m (ik)^{(15-m)}} \quad (47)$$

In order to ensure that limit of C'' approaches unity as k tends to zero, $b_{15} = 0.5 a_{15}$. It also should be noted that four additional real poles and zeros are added in order to model the branchcut. The coefficients $a_1 \dots a_{15}$, $b_1 \dots b_{14}$ are evaluated by minimizing the error function

$$E = \sum_{j=1}^{NFR} \left\| C''(ik_j, \bar{T}_{Re}, \bar{T}_{He}) - \frac{N(ik_j)}{D(ik_j)} \right\|^2 \quad (48)$$

This leads to a nonlinear least squares problem which converges rather slowly. The early numerical results for this case shows that this choice of error function provided more accurate approximations than an error function of the following form

$$E = \sum_{j=1}^{NFR} \left\| C'' D(ik_j) - N(ik_j) \right\|^2 \quad (49)$$

The coefficients calculated are summarized in Table I. In Figures 11 and 12 the real and imaginary parts of the approximate cascade lift deficiency function are compared with the corresponding exact values. The resulting agreement is very good up to $k=1.5$. However the procedure failed to model the very large peak and valley in the vicinity of $k=2.0$.

5. Concluding Remarks

A cascade wake theory was developed in the Laplace domain and was specialized to the frequency domain. A combined numerical and analytical scheme is developed to deal with various integrals and infinite summations involved. The influence of the number of the returning wake layers beneath the rotor is studied by presenting numerical examples.

The cascade wake model lift deficiency function in the frequency domain was compared with that of Loewy. It was found that the cascade wake theory predicts somewhat larger unsteady aerodynamic effects at integer frequency ratios than Loewy's theory. Furthermore the low reduced frequency limit of the cascade wake theory tends to the correct quasisteady limit, whereas Loewy's theory predicts very large reductions in loads near the zero reduced frequency.

Using a modified Pade approximant technique suitable for rotary wings, accurate finite-state time domain representation of cascade theory are developed. These time-domain models are useful for accurate modeling and design of active control systems used for vibration reduction or eliminating various type of instabilities such as ground resonance.

REFERENCES

1. Dinyavari, M.A.H., and Friedmann, P.P., "Unsteady Aerodynamics in Time and Frequency Domains for Finite Time Arbitrary Motion of Rotary Wings in Hover and in Forward Flight," AIAA Paper 84-0988, Proceedings AIAA/ASME/ASCE/AHS 25th Structures, Structural Dynamics and Materials Conference, Vol. II, May 1984, pp. 226-282.
2. Greenberg, J.M., "Airfoil in Sinusoidal Motion in Pulsating Stream," NACA TN 1326, 1947.
3. Dinyavari, M.A.H., and Friedmann, P.P., "Application of the Finite-State Arbitrary Motion Aerodynamics to Rotor Blade Aeroelastic Response and Stability in Hover and Forward Flight," AIAA Paper 85-0763, Proceedings AIAA/ASME/ASCE/AHS 26th Structures, Structural Dynamics and Materials Conference, to be published April 1985.
4. Loewy, R.G., "A Two-Dimensional Approximation to the Unsteady Aerodynamics of Rotary Wings," Journal of Aeronautical Sciences, Vol. 24, No. 2, February 1957.
5. Asghar-Hessari-Dinyavari, M., "Unsteady Aerodynamics in Time and Frequency Domains for Finite-Time Arbitrary-Motion of Helicopter Rotor Blades in Hover and Forward Flight," Ph.D. Dissertation, Mechanical, Aerospace and Nuclear Engineering Department, University of California, Los Angeles, California, March 1985.
6. Dowell, E.H., "A Simple Method for Converting Frequency Domain Aerodynamics to the Time Domain," NASA TM-81844, 1980.
7. Vepa, R., "Finite-State Modeling of Aeroelastic Systems," Ph.D. Dissertation, Department of Aeronautics and Astronautics, Stanford University, May 1975.
8. Friedmann, P.P. and Venkatesan, C., "Finite State Modeling of Unsteady Aerodynamics for Rotary Wings and Its Effect on Rotor Flapping Response," Eleventh European Rotorcraft Forum, September 1985, London, England.
9. Venkatesan, C., and Friedmann, P.P., "Finite State Modeling of Unsteady Aerodynamics and Its Application to a Rotor Dynamic Problem," University of California, Los Angeles, School of Engineering and Applied Science Report, UCLA-ENG-85-10, March 1985.
10. Hammond, C.E. and Pierce, G.C., "A Compressible Unsteady Aerodynamic Theory for Helicopter Rotors," AGARD Specialists Meeting on the Aerodynamics of Rotary Wings, Marseille, France, September 1972.
11. Johnson, W., Helicopter Theory, Princeton University, 1980.

Table I Coefficients of the Approximate Lift
Deficiency Function

N(ik)		D(ik)	
a ₁	0.449	b ₁	0.657
a ₂	1.25	b ₂	0.482
a ₃	0.0979	b ₃	0.573
a ₄	2.01	b ₄	1.09
a ₅	2.44	b ₅	1.22
a ₆	0.684	b ₆	0.883
a ₇	0.993	b ₇	0.558
a ₈	0.703	b ₈	0.970
a ₉	1.61	b ₉	1.48
a ₁₀	1.20	b ₁₀	1.02
a ₁₁	0.764	b ₁₁	0.135
a ₁₂	0.690	b ₁₂	0.560
a ₁₃	1.03	b ₁₃	0.610
a ₁₄	0.371	b ₁₄	0.285
a ₁₅	0.258	b ₁₅	0.129

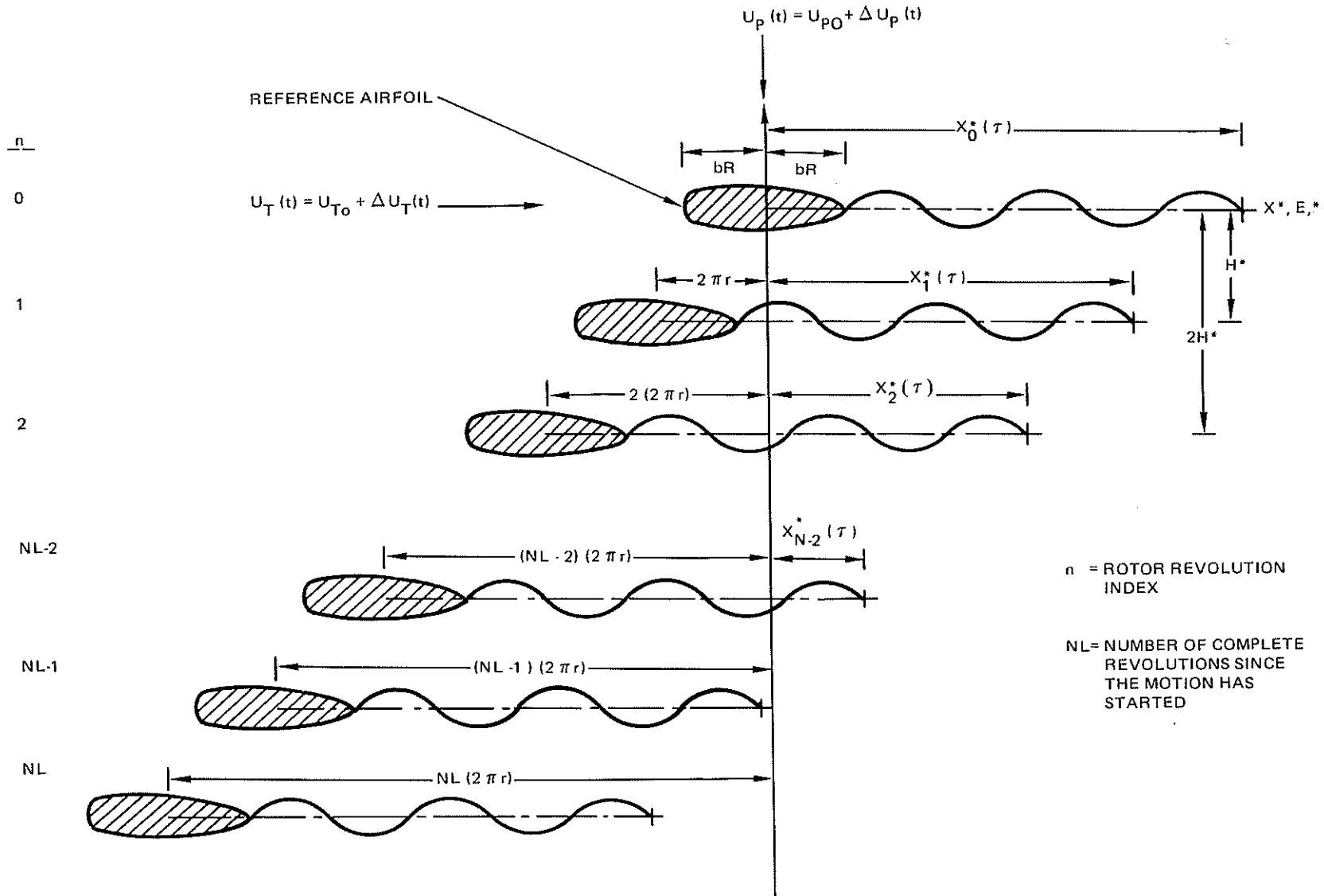
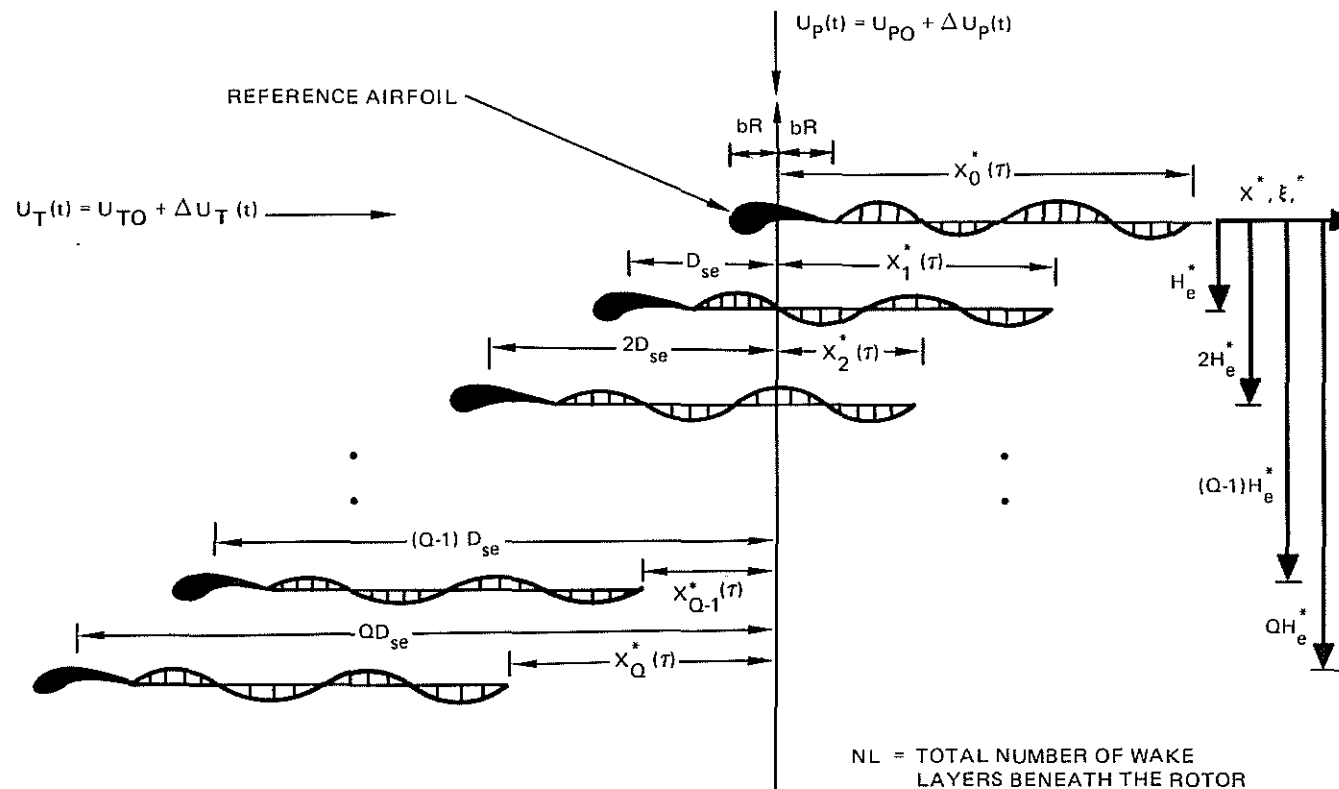


Figure 3. Schematic of the Cascade Wake Model for the Arbitrary-Motion Rotary-Wing Aerodynamic Theory in the Case of Single-Bladed Rotor

n	q	i
0	0	0
0	1	1
0	2	2
•	•	•
•	•	•
0'	Q-1	Q-1
1	0	Q
•	•	NL



- NL = TOTAL NUMBER OF WAKE LAYERS BENEATH THE ROTOR
- D_{se} = WAKE SHIFT BETWEEN SUCCESSIVE LAYERS: $(2\pi r) / Q$
- n = ROTOR REVOLUTION INDEX
- q = BLADE INDEX
- Q = NUMBER OF BLADES
- i = WAKE LAYER INDEX: $nQ+q$

Figure 4. Schematic of Cascade Wake Model for Arbitrary-Motion Rotary-Wing Aerodynamic Theory for the Multibladed Rotor

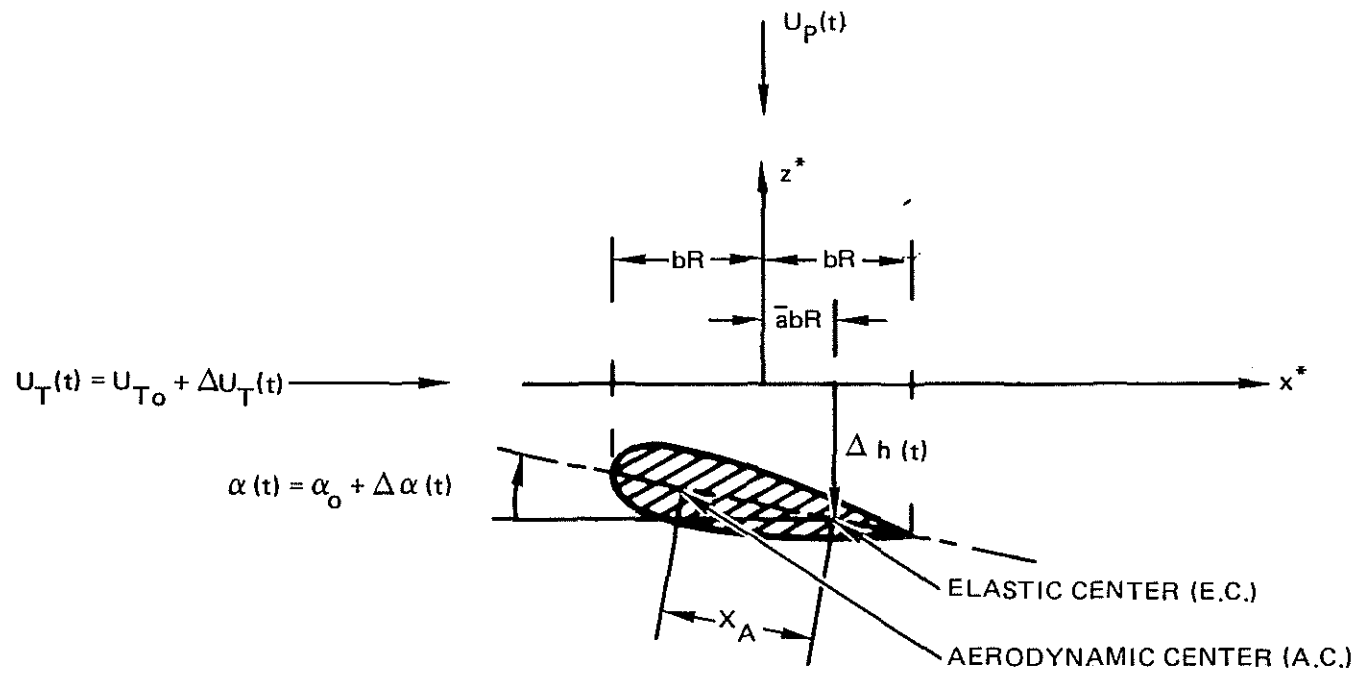
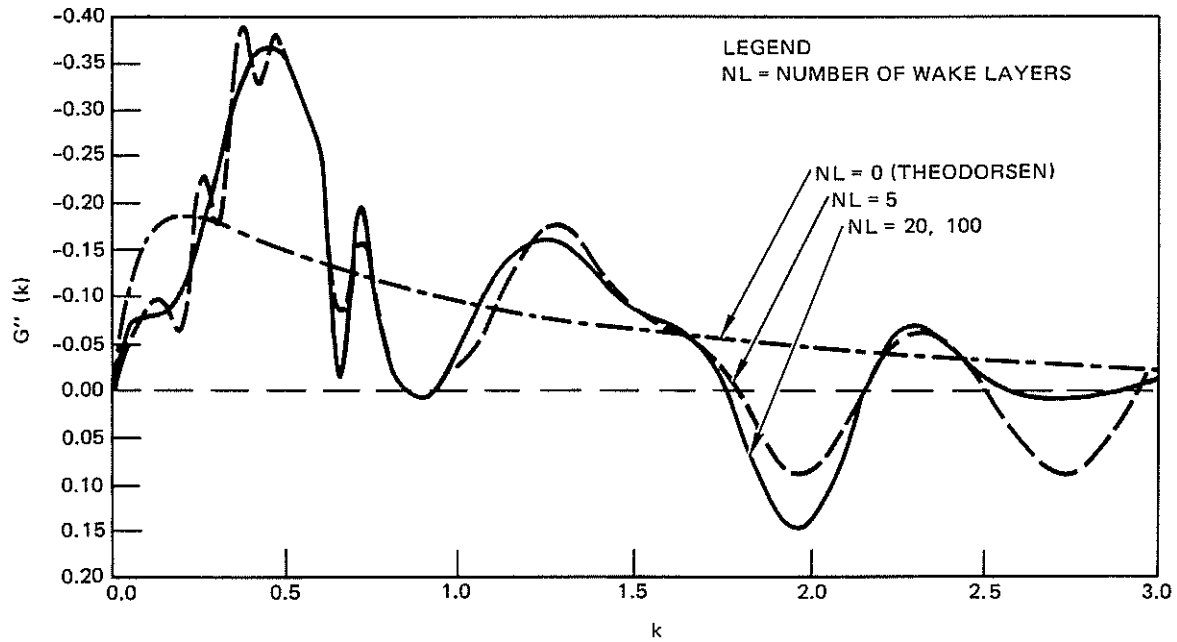
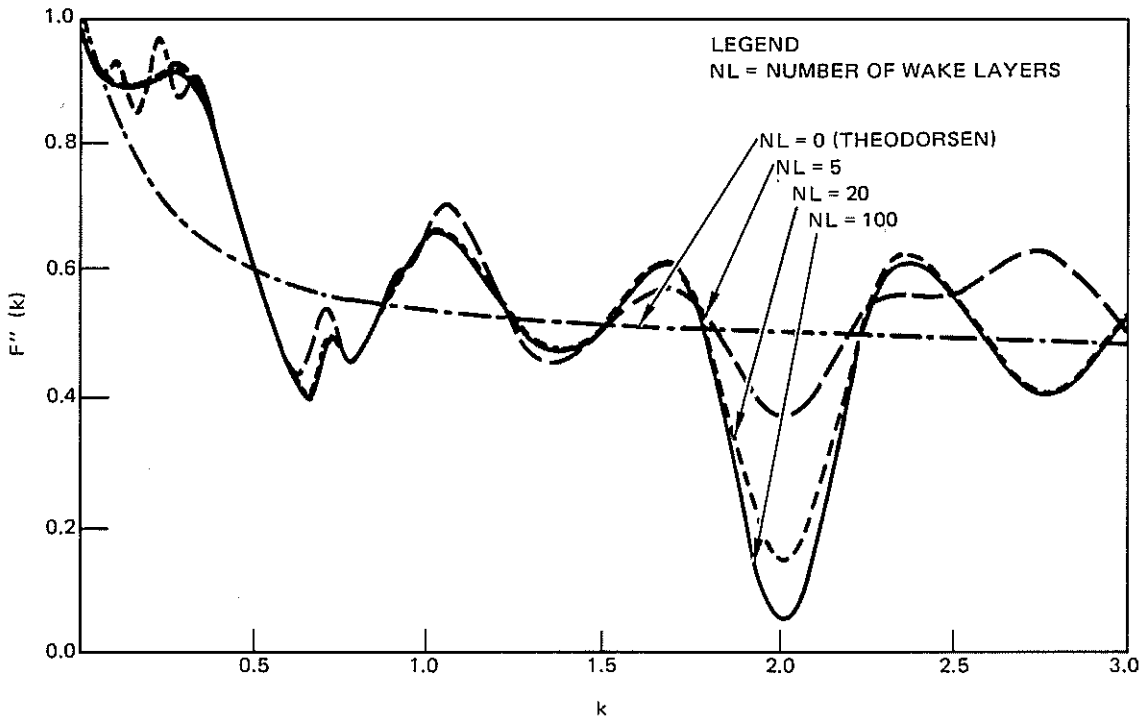
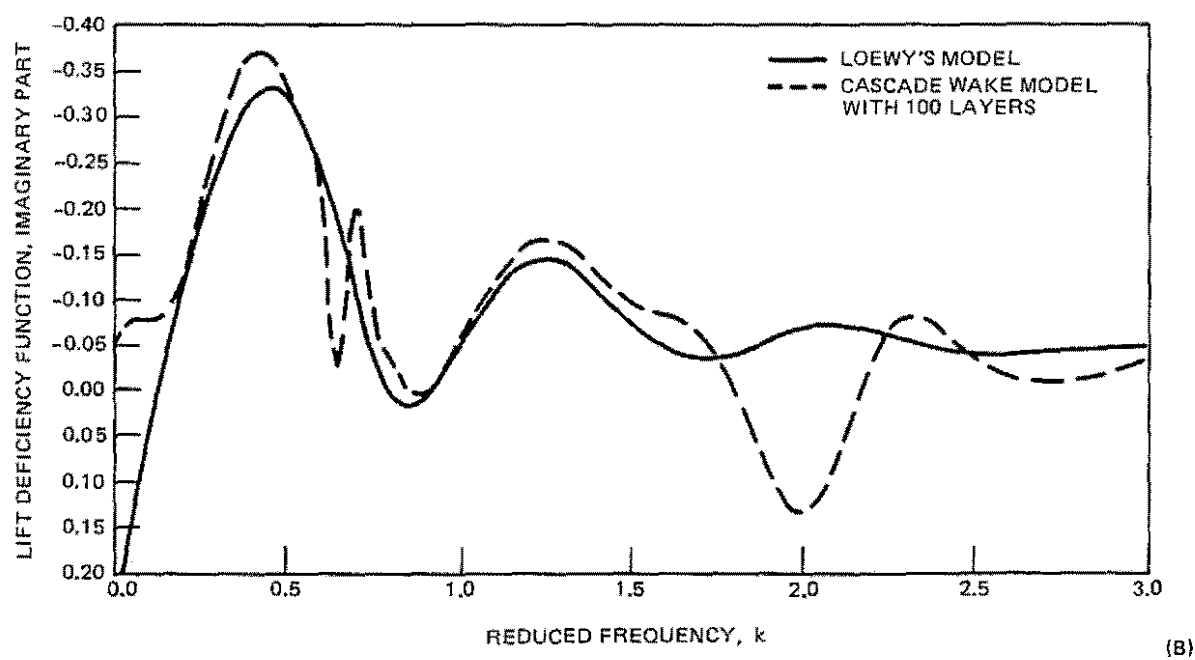
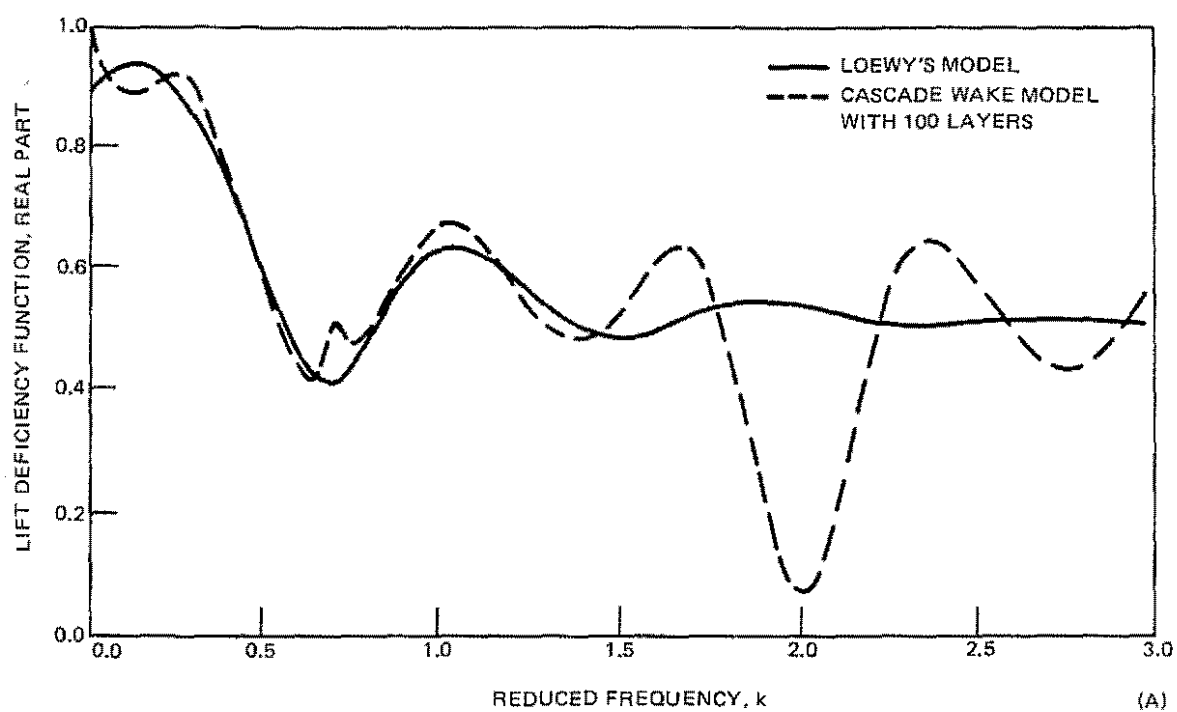


Figure 5. Geometry of Motion of a Typical Airfoil



Figures 6,7. Cascade Wake Model Lift Deficiency Function for Increasing Numbers of Wake Layers (for $\bar{T}_{Re} = 9.4248$, $\bar{T}_{He} = 1.5707$; $\bar{r}_e = 1.5$, $\bar{h}_e = 1.5707$)



Figures 8,9. Comparison of Cascade Wake Model and Loewy's Lift Deficiency Functions (for $\bar{T}_{Re} = 9.4248$, $\bar{T}_{He} = 1.5707$; $\bar{r}_e = 1.5$, $\bar{h}_e = 1.5707$)

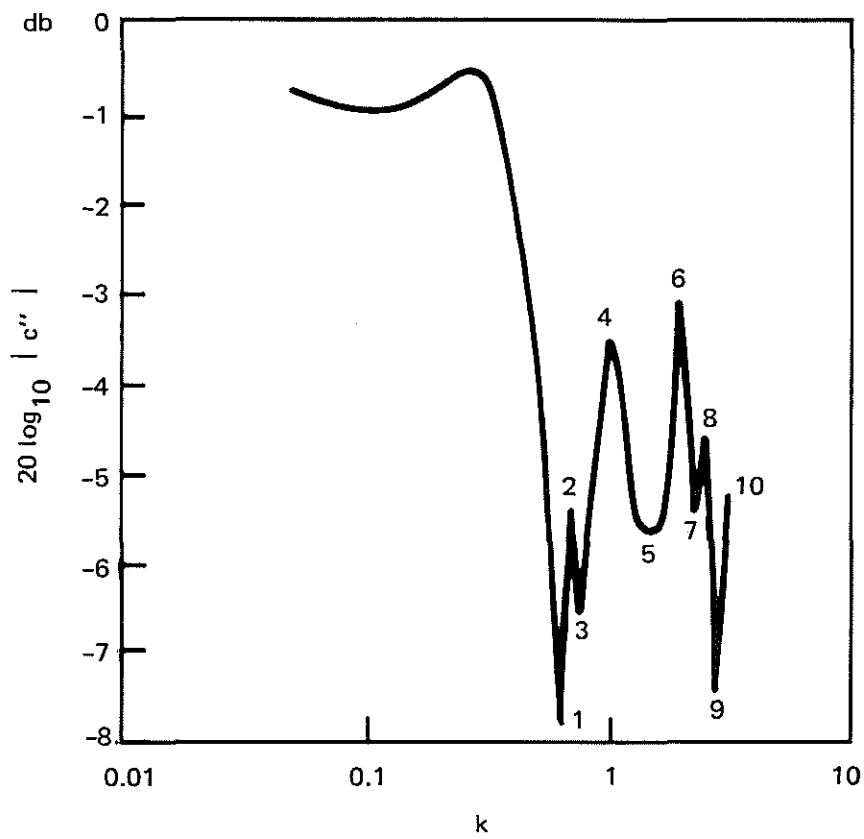
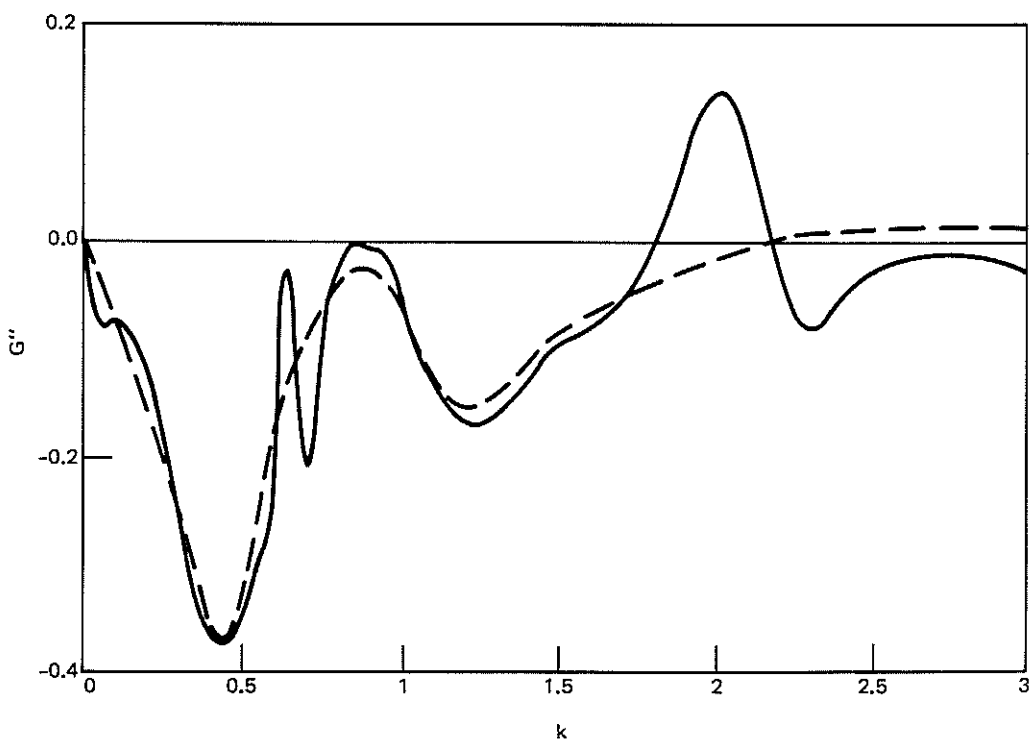
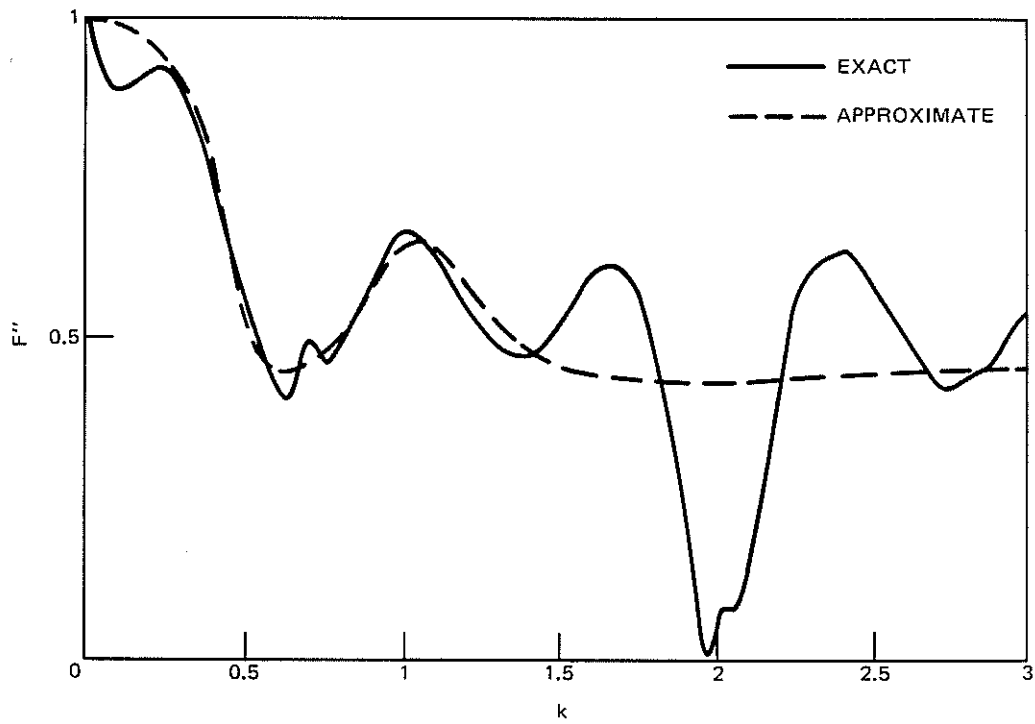


Figure 10. Bode Plot of Cascade Lift Deficiency
 Function for $\bar{T}_{He} = 1.5707$, $\bar{T}_{Re} = 9.4248$



Figures 11, 12. Cascade Lift Deficiency Function and its 15th Order Complex Pade Approximant for $\bar{T}_{He} = 1.5707$, $\bar{T}_{Re} = 9.4248$ (Coefficients of Pade Approximant are given in Table 1)